Accurate local region prediction by precise motion model in Kalman-particle filter

Xu Chao[1], Gao Min[1], Yang Yao[2]

(1. Missile Engineering Department, Ordnance Engineering College, Shijiazhuang 050003, China;
2. Chongqing Optoelectronics Research Institute, Chongqing 400060, China)

Abstract: Particle filter is widely used for visual tracking with superior performance in terms of accuracy and robustness, but it suffers from the heavy computational load, and the calculation complexity increases quickly with the state dimension and the number of particles. In this paper, the tracking problem was considered as a coarse-to-fine process to find the optimal state, thus, a hierarchical Kalman-particle filter (HKPF) with precise motion model, called improved hierarchical Kalman-particle filter (IHKPF), was proposed, in which Kalman filter with Jerk model was used to predict a local region around the estimation of global linear motion, and then particles were generated in the local region. The reason for introducing Jerk model was that the inadequate tracking performance of current models with the higher order derivating in the case of very highly maneuvering targets were not tracked therefore, Jerk was added. The high order state variable Jerk was applied in motion model of IHKPF. The HKPF, PF and proposed in the paper were used to compelete track experiment. The experimental results among the proposed algorithm HKPF and PF indicate that Jerk model provides higher accuracy prediction, resulting in well- behaved tracking in complex environment.

Key words: improved hierarchical Kalman-particle filter; coarse-to-fine; region estimation; Jerk model

CLC number: TP391 **Document code:** A **Artide ID:** 1007-2276(2015)11-3475-08

卡尔曼粒子滤波中基于精确运动模型的局部区域估计

徐 超[1],高 敏[1],杨 耀[2]

(1. 军械工程学院 导弹工程系, 河北 石家庄 050003; 2. 重庆光电技术研究所, 重庆 400060)

摘 要: 粒子滤波广泛应用于对精度和稳定性要求较高的目标跟踪,但其计算量大,并且计算复杂度随着状态量和粒子数目增长迅速增加。将目标跟踪转化为由粗到精的搜索过程,提出了一种基于精确运动模型的改进分层卡尔曼粒子滤波算法。该方法利用加速度的运动模型在真实目标位置的周围估计目标的散布范围,并在该范围内随机生成粒子,寻找精确的目标位置。文中引入加加速度模型主要是由于现有方法的状态量阶数不足,导致模型精确度较低,无法应对大机动目标的跟踪。因此,引入

收稿日期:2015-03-13; **修订日期**:2015-04-15

基金项目:军内科研项目;军械工程学院科研基金(YJJM11018)

作者简介:徐超(1987-),男,博士生,主要从事计算机视觉及图像末制导技术方面的研究。Email: 475084845@qq.com

导师简介:高敏(1963-),男,教授,博士生导师,博士,主要从事计算机视觉及图像末制导技术方面的研究。
Email: gaomin1103@gmail.com

了高阶状态变量加加速度,并将其用于改进分层卡尔曼粒子滤波的运动模型。利用分层卡尔曼粒子滤波、粒子滤波以及提出的方法进行了跟踪试验,结果表明,基于精确运动模型的改进分层卡尔曼粒子滤波模型的跟踪方法能够提高线性运动的预测精度,实现复杂环境下精确稳定的跟踪。

关键词:改进分层卡尔曼粒子滤波; 由粗到精搜索策略; 区域估计; Jerk 模型

0 Introduction

Visual tracking plays a critical role in video-based computer vision applications, ranging from operation monitoring, intelligent video surveillance, human-computer interaction, and augmented reality to automatic drive, robotics or medical assistances [1]. However, visual tracking of object in complex environments remains a lot of difficulties caused by the dynamic change in object/background appearance, abrupt motion, illumination changes, and total or partial occlusion. Moreover, it is also required that tracking must be performed reliably over very long sequences and operated at high frame rates.

Numerous tracking approaches [2-6] have been proposed for better performance in the past two decades. A detailed survey is shown in reference [7]. Researchers have fallen into three different categories to deal with the tracking problem, namely appearance models [8], motion models [9] and searching strategies [10]. Appearance model is applied to discriminate the object with its background during all the tracking process. It is required absolutely discriminative, computationally efficient and adaptive to achieve very good tracking results. Unfortunately, developing such a perfect appearance model is rather difficult until now. Hence, considerable effort should be made for novel appearance models. On the other hand, motion models are employed to predict the object´s location in a new frame within a video sequence based on its history motion characteristics. A well-performed motion model can improve the tracking stabilization, reduce the searching areas of the state, and make the tracking survive from occlusions could not be obtained[11]. But an accurate motion model could not be obtained especially in adverse conditions such as nonlinearity and non-Gaussian, and the estimation may be located in the wrong area. To solve the problem, *m*-order Markov chain models[12], autoregressive process[13], etc. are proposed. As a special case, HKPF [14] partition the object motion into the global part and local part solving by constant acceleration model and Brownian motion, respectively. This hierarchical strategy introduces a novel issue for proper motion model. In the dynamic process, KF with constant acceleration model is introduced. The algorithm obtains an efficient prediction under such an assumption that abrupt motion of target can be regarded as smooth motion with high enough sampling frequency. However, high frequency frames for dealing with dramatic motion change will bring computational load in real time tracking, and image grabbing of actual scenario at super-high frequency is also difficult for most application. Thus, Jerk model is applied to instead of constant acceleration model for maneuver tracking without super-high frequency frames. As described in [15], the reason for the inadequate tracking performance of current models is that the higher order derivating in the case of very highly maneuvering targets are not insignificant, leading to model inaccuracies when terms only up to the second order are included. Therefore, t he third order position derivative, jerk is added and the improved hierarchical Kalman-particle filter with precise motion model is proposed.

The remainder of this paper is organized as follows. Section 1 gives the detail of position estimation in coarse estimation. The region estimation in coarse estimation is discussed in Section 2. To simplify, fine estimation is not repeat again, and the detail is referring to[14]. Experimental results are presented in Section 3 with various examples and quantitative analysis. Section 4 concludes this paper.

1 Position estimation

Coarse estimation is composed by two parts: position estimation and region estimation. The purpose of the

former is to track the linear component of object motion in the global view. The discrete state transition equation is expressed as follows:

$$X_k=FX_{k-1}+\varepsilon_k \tag{1}$$

The corresponding measurement equation is

$$Z_k=HK_{k-1}+\tau_k \tag{2}$$

Where ε_k, τ_k represents the process and measurement noise at time index k respectively. Herein, ε_k and τ_k are assumed to be zero-mean Gaussian noise. F and H are the state transition matrix and measurement matrix, respectively.

$$F=\begin{bmatrix} 1 & 0 & T & 0 & T^2/2 & 0 & p & 0 \\ 0 & 1 & 0 & T & 0 & T^2/2 & 0 & p \\ 0 & 0 & 1 & 0 & T & 0 & q & 0 \\ 0 & 0 & 0 & 1 & 0 & T & 0 & q \\ 0 & 0 & 0 & 0 & 1 & 0 & r & 0 \\ 0 & 0 & 0 & 0 & 0 & 1 & 0 & r \\ 0 & 0 & 0 & 0 & 0 & 0 & S & 0 \\ 0 & 0 & 0 & 0 & 0 & 0 & 0 & S \end{bmatrix} \tag{3}$$

$$H=\begin{bmatrix} 1 & 0 & 0 & 0 & 0 & 0 & 0 & 0 \\ 0 & 1 & 0 & 0 & 0 & 0 & 0 & 0 \end{bmatrix} \tag{4}$$

F indicates Jerk model and H implies that only positional elements are measurable. p, q, r, s are the dependent variables of the sampling period T and the reciprocal of the jerk time constant. The equations are as follows

$$p=(2-2\alpha T+\alpha^2T^2-2e^{-\alpha T})/(2\alpha^3) \tag{5}$$

$$q=(e^{-\alpha T}-1+\alpha T)/\alpha^2 \tag{6}$$

$$r=(1-e^{-\alpha T})/\alpha \tag{7}$$

$$S=e^{-\alpha T} \tag{8}$$

Given a fixed time period T, the state transition matrix F might be changed as time goes by because of the alternation of time constantin Jerk model. Certainly, target maneuver is set to an accident in our real tracking, and the Jerk model is reduced to constant acceleration model in most cases unless dramatic motion. Accordingly, F is almost a constant and sometimes adaptive to maneuver for an accurate prediction. The time of the coarse estimation is one step behind the system time because the measurement Z_k of Kalman filter is approximated by Z_k^* extracted from the output of PE framework at time k. The prediction and updating in our implementation is as follows:

$$\hat{X}_{k-1}=Fx_{k-2} \tag{9}$$

$$\hat{\Sigma}_{k-1}=F\Sigma_{k-2}F_{k-1}^{\mathrm{T}}+R_{k-1} \tag{10}$$

$$K_{k-1}=\Sigma_{k-1}H^{\mathrm{T}}(H\Sigma_{k-1}H^{\mathrm{T}}+Q_{k-1})^{-1} \tag{11}$$

$$X_{k-1}=X_{k-1}+K_{k-1}(Z_{k-1}^*-HX_{k-1}) \tag{12}$$

$$\Sigma_{k-1}=(I-K_{k-1}H)\Sigma_{k-1} \tag{13}$$

Here, R_{k-1} and Q_{k-1} are defined as the corresponding covariance of ε_k and τ_k respectively based on the assumption of Gaussian noise. Σ_k denotes the covariance of states. Eqs. (9) and (10) are the prediction step of Kalman filter, and K_{k-1} in Eq. (11) is the Kalman gain. Eqs. (12) and (13) are the updating step of Kalman filter. Z_{k-1}^* in Eq. (11) is obtained by the fine estimation described below. The final output of Kalman filter is the global motion state, which represents the actual global motion state at a maximum probability under the assumption of the linear Gaussian motion. Given the global motion state at time $k-1$ and state transition equation, the prediction of the next position and the global displacement is obtained:

$$X_k=FX_{k-1} \tag{14}$$

$$d_k^g=H(X_k-X_{k-1})=\begin{bmatrix} \triangle x_k^g \\ \triangle y_k^g \end{bmatrix} \tag{15}$$

As described in Eqs. (15), the global displacement d_k^g is a 2×1 vector and defined by $[\triangle x_k^g \ \triangle y_k^g]$, where $\triangle x_k^g$, $\triangle y_k^g$ represent the global displacement along horizontal and vertical coordinate at time k, respectively.

2 Region estimation

KF with Jerk model could predict the coarse position of target and the truth is located at the area around the prediction. Commonly, Jerk model is degenerated into constant acceleration model without abrupt motion. Thus, the covariance of normal distribution, i.e., the proposal

distribution of random particles for fine estimation is determined by a constant ψ_C and ψ_{Σ_k}. ψ_C is the diagonal covariance matrix whose elements are the minimum variance of the affine parameter. ψ_{Σ_k} is the Gaussian distribution of the positional elements of M_{k-1}, which comes from the estimation of KF and is defined by extracting the positional covariance from Σ_k.

$$\psi_C=\begin{bmatrix}\sigma_s^2&0&0&0&0&0\\0&\sigma_a^2&0&0&0&0\\0&0&\sigma_\theta^2&0&0&0\\0&0&0&\sigma_\phi^2&0&0\\0&0&0&0&\sigma_x^2&0\\0&0&0&0&0&\sigma_y^2\end{bmatrix} \tag{16}$$

$$\psi\Sigma_k=C^{\mathrm{T}}(H\Sigma_k H^{\mathrm{T}})C=\begin{bmatrix}0&0&0&0&0&0\\0&0&0&0&0&0\\0&0&0&0&0&0\\0&0&0&0&0&0\\0&0&0&0&\sigma_{x_k^2}&\sigma_{x_k y_k}\\0&0&0&0&\sigma_{y_k x_k}&\sigma_{y_k^2}\end{bmatrix} \tag{17}$$

Where

$$C=\begin{bmatrix}0&0&0&0&1&0\\0&0&0&0&0&1\end{bmatrix} \tag{18}$$

The distribution of particles is fixed soon because ψ_C is predefined and ψ_{Σ_k} would converge to a constant covariance matrix after several time intervals, even there is a little change in ψ_{Σ_k} with abrupt motion, because target maneuver just occurs in a short time. However, a region that could adapt to the target's significant motion changes is expected for generating random samples. Like the hypothesis in reference [11], acceleration in our coarse estimation is assumed constant because Jerk model is degenerate in most cases and the violation only occurs when the force applied to the object is changed. Hence, we address the change of acceleration with a similar manner, i.e. an adaptive region estimation method to maintain a dynamic elliptical region for capturing motion changes. The elliptical region corresponds to the Gaussian distribution which can be configured by a 2×2 covariance matrix. We define ψ_{D_k} to represent the dynamic portion of covariance matrix at time. In this process, the direction and length of axes for elliptical region need to be determined. For the direction, we only need to address the major axis because the minor axis is perpendicular to it. Similarly, we just also calculate the length of the major axes because another is tightly dependent.

For the purpose of modeling the nonlinear uncertainty by elliptical Gaussian distribution, the mathematical procedure is given to construct the corresponding covariance matrix. The procedure of natural abrupt motion is composed of ascent process, peak process and descent process (shown in Fig.1). Usually the peak process is very short in time, while the ascent process and descent process relatively takes a long time. Then the difference in acceleration is proportional to the strengths of nonlinearities and non-Gaussian statistics caused by motion change, which means their difference proportional to the degree of force changing by Newton's second law. Thus the maximal displacement by nonlinear uncertainty during the time from $k-1$ to can be calculated by

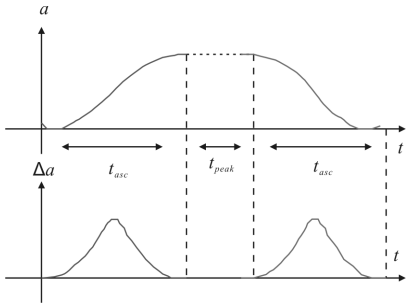

Fig.1 Alteration of acceleration under abrupt motion

$$d_k^d=\frac{1}{2}\Delta a_{k-1}T^2=\begin{bmatrix}\Delta x_k^d\\ \Delta y_k^d\end{bmatrix} \tag{19}$$

Where

$$\Delta a_{k-1}=\begin{bmatrix}\ddot{x}_{k-1}-\ddot{x}_{k-2}\\ \ddot{y}_{k-1}-\ddot{y}_{k-2}\end{bmatrix} \tag{20}$$

The maximal displacement by nonlinear uncertainty

d_k^d and the global displacement d_k^g in Eqs. (15) are complementary. In other words, d_k^g represents the linear prediction of the global displacement, and d_k^d denotes the maximal nonlinear prediction of the local displacement. Then, the maximum of the total displacement vector can be defined and calculated as follow

$$V_k = d_k^g + d_k^d \tag{21}$$

V_k means the maximal region of target maneuver, but such an irregular vector could not describe the Gaussian distribution directly. Therefore, an ellipse is chosen to approximate the maximal region, and the direction of major axis is equal to the direction of V_k, calculated as

$$\theta_k = \arctan\left(\frac{\Delta y_k^g + \Delta y_k^d}{\Delta x_k^g + \Delta x_k^d}\right) \tag{22}$$

Certainly, the length of major axis is also set to be the same as $||V_k||$ to cover the maximal displacement region, calculated as

$$\sigma_k^{major} = ||V_k|| = \sqrt{\left(\Delta x_k^g + \Delta x_k^d\right)^2 + \left(\Delta y_k^g + \Delta y_k^d\right)^2} \tag{23}$$

As mentioned above, the direction of minor axis is perpendicular to the one of major axis, defined as φ_k. When it comes to the length, the minor axis is often proportional to the major axis to tolerate the off-major axial nonlinear noise. A proper ratio is critical, because too small a ratio could not cover the maximal displacement region with weakness to off-major axial noise while too large a ratio would significantly enlarger the particles distribution region resulting in much useless calculation. We set the ratio in a range, and the final value of ratio is depending on two factors. One is the uncertainty of motion, i.e., the ratio will increase while target maneuver drastically; another is to be sure the density of particle along the major axis enough, which means the ratio will decrease while the major axis grow. In experience, the range of the ratio is choose as follow

$$\sigma_k^{minor} / \sigma_k^{major} = \frac{1}{3} \sim \frac{1}{4} \tag{24}$$

To date, we obtain complete parameters of the dynamic ellipse region, and could construct the covariance matrix ψ_{D_k}. In this process, the principle of Singular Value Decomposition (SVD) is applied to decompose ψ_{D_k} into three parts. The physical meaning of SVD decomposition of can be regarded as the geometric transformation relative to unit circle: rotation (by φ_k), stretching (the changes of the length of major axis and minor axis) and finally another rotation (by θ_k). Each transformation in the decomposition corresponds to a matrix. Note that, the matrix for describing unit circle is a 2D identity matrix. Thus, after neglecting identity matrix, the concatenation of all transformation matrixes in sequence builds the covariance matrix. The rotation matrix of by φ_k and another matrix by θ_k are inverses of each other because θ_k and φ_k are perpendicular. The former rotation matrix is configured by

$$Rot_k = \begin{bmatrix} \cos\varphi_k & -\sin\varphi_k \\ \sin\varphi_k & \cos\varphi_k \end{bmatrix} \tag{25}$$

The stretching matrix is a diagonal matrix, and its diagonal terms are configured by the lengths of the major axis and the minor axis

$$D_k = \begin{bmatrix} \left(\sigma_k^{major}\right)^2 & 0 \\ 0 & \left(\sigma_k^{minor}\right)^2 \end{bmatrix} \tag{26}$$

ψ_{D_k} can be computed as

$$\psi_{D_k} = Rot_k D_k Rot_k^{-1} \tag{27}$$

Thus, the final covariance matrix for random-walk dynamic model can be redefined by

$$\psi_k = (1 - m_k) \cdot (\psi_C + \psi_{\Sigma_k}) + m_k \cdot C^T \psi_{D_k} C \tag{28}$$

Where, m_k is the weight between ψ_k's static part and dynamic part.

3 Experimental results

3.1 Experimental setup

Experiments are implemented on two sequences to verify the effectiveness and efficiency of the proposed algorithm. The videos are "Motor Rolling" and "Jumping". For "Motor Rolling" sequence, the comparison of Jerk model adopted by our algorithm and the constant

acceleration model in HKPF is executed to evaluate the goodness-of-fit of our motion model. In "Jumping", we employ improved HKPF, HKPF and PF for real tracking and analyze the experimental results to find well-behaved tracking algorithm under these different circumstances. Parameters of HKPF and improved HKPF are self-adaptive except for the constant diagonal covariance matrix ψ_C. Thus we assign $\psi_{C1}=diag\ (0.03^2, 0.001^2, 0.03^2, 0.1^2, 4^2, 4^2)$ for constant acceleration model and $\psi_{C2}=diag\ \ (0.03^2, 0.001^2, 0.03^2, 0.1^2, 2^2, 2^2)$ for Jerk model. All experiments are performed at the same platform, which uses Intel 2.5 GHz CPU and 4 GB memory, and the tests are executed under Windows XP+MATLAB 2011b.

Since motion model determines the accuracy of position prediction and the size of local region, we study the performance of existing models and introduce Jerk model with higher order derivatives instead of constant acceleration model to address target maneuver without superhigh frequency frames. With these two models, HKPF and improved HKPF are both used for state estimation of target in "Motor Rolling" sequence. Fig.2 describes motor motion and the predictions by constant acceleration model and Jerk model. As shown in Fig.2 (a), the prediction of constant model could follows the target tightly and reduce the search area to some extent. But the sudden raising maneuver is not treated perfectly. Fig.2(b) gives an ideal position estimation, in which the predictions are closer to ground truth, even goes by dramatic motion. Thus the minimum variances of horizontal and vertical translations in ψ_{C2} are smaller than those in ψ_{C1}. Similarly, another two terms of ψ_k (shown in Eq.28) are both falling down because the Jerk model´s trajectory is smooth relative to constant acceleration model. Given local regions, PF is applied to generate a small number of particles respectively and the final tracking results are shown in Fig.3. The adaptive region ellipse in each frame

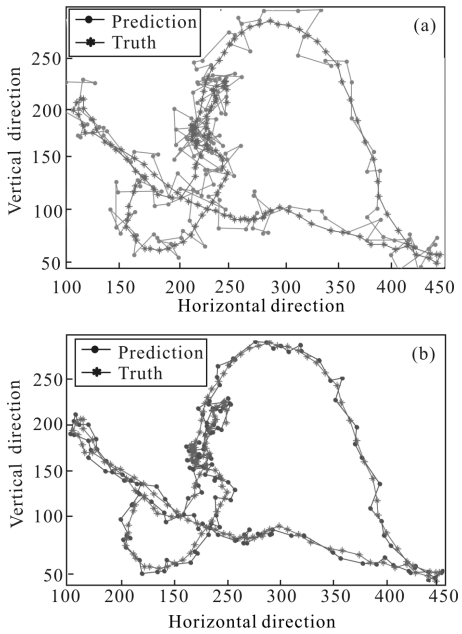

Fig.2 Motor motion and the predictions by constant acceleration model and Jerk model: (a) comparison of ground truth and the prediction of constant acceleration model; (b) comparison of ground truth and the prediction of Jerk model

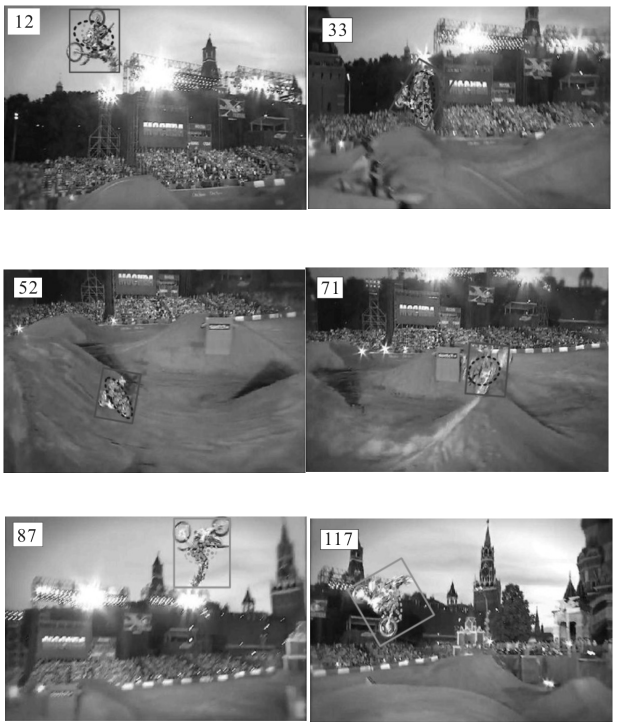

(a) HKPF with 20 particles

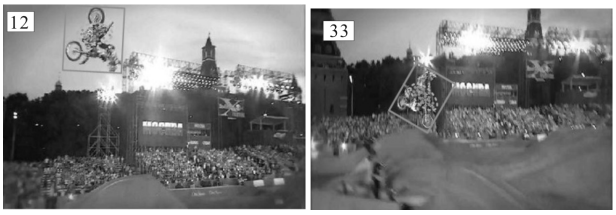

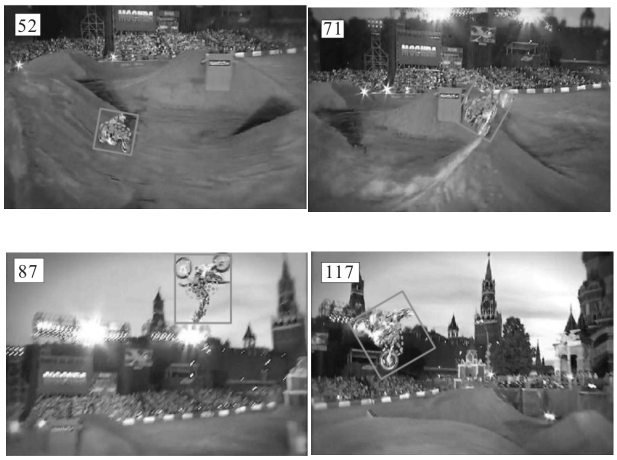

(b) Improved HKPF with 20 particles

Fig.3 Comparison of improved HKPF and HKPF under dramatic motion in "Motor Rolling" sequence. In each image frame, green or red quadrilateral box is the estimated tracking box; cyan or blue ell ipse indicates the estimated elliptical proposal distribution; each green point corresponds to a particle

is drawn to show how ψ_k varies dynamically under rapid motion changes by different algorithms. In the comparison, improved HKPF shows super performance on position tracking, even higher accuracy of scale and orientation. The reason is that all samples are generated pseudo-randomly. The particles in HKPF near true pose maybe located at wrong position, while others stayed at right position would be far away from proper pose. Improved HKPF solve this problem by reducing the ellipse region. More particles are close to ground truth and the distribution of pose parameters is available, resulting in accurate pose tracking.

"Jumping" sequence is introduced to further evaluate the performance of our algorithm, which is showing shuttling, camera motion and blurring, which means man in this sequence undergoes complicated maneuver. Since PF, HKPF and IHKPF are all stochastic methods, there exists randomness in their tracking results, which implies that the results on the same video sequence vary from time to time without parameter change. To insure fairness in our experiment, all tracking algorithms run one hundred times with mutual different random seeds on each video sequence. Moreover, their results are compared in a statistical way. Video sequences have ground truths that record object's position using 2D point at each image frame. The tracking error at each frame between tracking result and ground truth is measured by root mean square error (RMSE) and calculated as follows:

$$RMSE(t)=\sqrt{\left(\hat{C}_t(x)-C_t(x)\right)^2+\left(\hat{C}_t(y)-C_t(y)\right)^2} \quad (29)$$

Where, $\hat{C}_t(x,y)$ and $C_t(x,y)$ are the center of the tracking window and the ground truth, respectively.

Tracking results of "Jumping" sequence are shown in Fig.4. PF could not address this video and quickly loses

Fig.4 Tracking results by improved HKPF (solid box), HKPF (dashed box) and PF (dotted box) on "Jumping" sequence

the target at frame #90 when blurring image occurs. HKPF tracks the head robustly but many particles are inevitable, consuming an average of 42.5 particles per frame in this sequence. As comparison, improved HKPF achieves better performance to various challenges with only 31.2 particles per frame for average. The RMSEs of the three trackers (i.e., PF, HKPF, and IHKPF) between the

estimated location of the targets center and the ground truths are shown in Fig.5. The RMSE of PF tracker is larger than other two algorithms, and not shown after frame #116 because it loses the target absolutely at that time due to large target motions. The RMSE curve of HKPF shows that, although it consumes more particles, the tracking performance still weaker than IHKPF. The average runtimes of tracking "Jumping" sequence by PF, HKPF, and IHKPF at our platform are shown in Tab.1. The calculations of HKPF and IHKPF are decreased dramatically comparing with PF, especially IHKPF cost only 0.0472 s per frame. That means our algorithm could achieve real-time tacking while tracking accuracy over performs other two trackers.

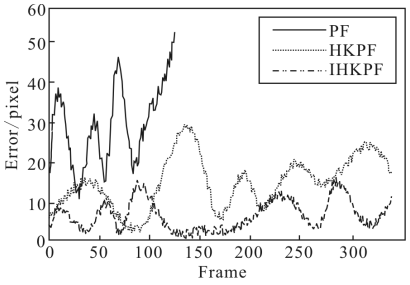

Fig.5 Comparisons of RMSE among PF, HKPF, and IHKPF

Tab.1 Comparison of average run time for "Jumping" sequence

	PF	HKPF	IHKPF
Runtime(116 frames)/s	0.2136	0.0624	0.0433
Runtime(total)/s	NAN	0.0699	0.0472

4 Conclusion and future work

Considering the advantages of Jerk model, we propose an algorithm called improved hierarchical Kalman - particle filter with precise motion model for efficient visual tracking. Jerk model is introduced to update the constant acceleration model for more precise prediction to improve the performance of tracking algorithm. The detail analysis of our algorithm and other approaches is implemented, and experimental results show that, the novel motion model is available with higher prediction accuracy.

The performance of motion model determines the accuracy of position prediction and the distribution of particles. Hence, we intent to study cubature Kalman filters for better prediction.

References:

[1] Martínez A, Jiménez J J. Tracking by means of geodesic region models applied to multidimensional and complex medical images [J]. ***Computer Vision and Image Understanding***, 2011, 115: 1083-1098. (in Chinese)

[2] Comaniciu D, Ramesh V, Meer P. Kernel-based object tracking [J]. ***IEEE Trans Pattern Anal Mach Intell***, 2003, 25(5): 564-577. (in Chinese)

[3] Avidan S. Ensemble tracking [J]. ***IEEE Trans Pattern Anal Mach Intell***, 2007, 29(2): 261-271. (in Chinese)

[4] Tian Li, Zhou Fugen, Meng Cai. Parallel particle filter object tracking based on embedded multi-core DSP systems [J]. ***Infrared and Laser Engineering***, 2014, 43(7): 2354-2361. (in Chinese)

[5] Cao Yang, Zhao Mingfu, Luo Binbin, et al. Airborne platform's tracking algorithm for free space optical [J]. ***Infrared and Laser Engineering***, 2012, 41(11): 3065-3068. (in Chinese)

[6] Li Quan, Zhao Xunjie, Peng Qingyan, et al. Windows adaptive particle filter algorithm based on principal component analysis [J]. ***Infrared and Laser Engineering***, 2014, 43(10): 3474-3479. (in Chinese)

[7] Yilmaz A, Javed O, Shah M. Object tracking: A survey [J]. ***ACM Comput Surv***, 2006, 38(4): 1-45. (in Chinese)

[8] Wang H, Suter D, Schindler K, et al. Adaptive object tracking based on an effective appearance filter [J]. ***IEEE Tran Pattern Anal Mach Intell***, 2007, 29(9): 1661-1667. (in Chinese)

[9] Bimbo A D, Dini F. Particle filter-based visual tracking with a first order dynamic model and uncertainty adaptation [J]. ***Computer Vision and Image Understanding***, 2011, 115: 771-786. (in Chinese)

[10] Zivkovic Z, Cemgil A T, Kröse B. Approximate Bayesian methods for kernel-based object tracking [J]. ***Computer Vision and Image Understanding***, 2009, 113: 743-749. (in Chinese)

[11] Isard M, Blake A. CONDENSATION - conditional density propagation for visual tracking [J]. ***International Journal on Computer Vision***, 1998, 29: 5-28. (in Chinese)